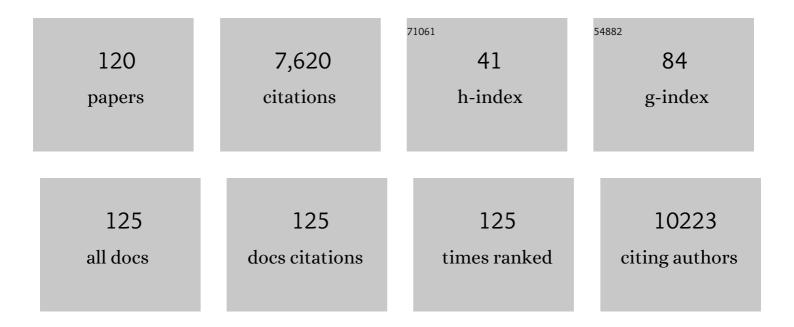
Jian-guo Wang

List of Publications by Year in descending order

Source: https://exaly.com/author-pdf/8325910/publications.pdf Version: 2024-02-01



Ιμανι-ςμο Μλαίς

#	Article	IF	CITATIONS
1	Balancing surface adsorption and diffusion of lithium-polysulfides on nonconductive oxides for lithium–sulfur battery design. Nature Communications, 2016, 7, 11203.	5.8	1,136
2	Size-Dependent Electrocatalytic Reduction of CO ₂ over Pd Nanoparticles. Journal of the American Chemical Society, 2015, 137, 4288-4291.	6.6	929
3	Hierarchical Porous NC@CuCo Nitride Nanosheet Networks: Highly Efficient Bifunctional Electrocatalyst for Overall Water Splitting and Selective Electrooxidation of Benzyl Alcohol. Advanced Functional Materials, 2017, 27, 1704169.	7.8	267
4	Pd-Containing Nanostructures for Electrochemical CO ₂ Reduction Reaction. ACS Catalysis, 2018, 8, 1510-1519.	5.5	261
5	Efficient Activation of Li ₂ S by Transition Metal Phosphides Nanoparticles for Highly Stable Lithium–Sulfur Batteries. ACS Energy Letters, 2017, 2, 1711-1719.	8.8	252
6	Switchable CO2 electroreduction via engineering active phases of Pd nanoparticles. Nano Research, 2017, 10, 2181-2191.	5.8	208
7	Synergistic effect of surface oxygen vacancies and interfacial charge transfer on Fe(III)/Bi2MoO6 for efficient photocatalysis. Applied Catalysis B: Environmental, 2019, 247, 150-162.	10.8	185
8	Mo Doping Induced More Active Sites in Urchinâ€Like W ₁₈ O ₄₉ Nanostructure with Remarkably Enhanced Performance for Hydrogen Evolution Reaction. Advanced Functional Materials, 2016, 26, 5778-5786.	7.8	177
9	Microporous 3D Covalent Organic Frameworks for Liquid Chromatographic Separation of Xylene Isomers and Ethylbenzene. Journal of the American Chemical Society, 2019, 141, 8996-9003.	6.6	171
10	Oxygen vacancies on TiO ₂ promoted the activity and stability of supported Pd nanoparticles for the oxygen reduction reaction. Journal of Materials Chemistry A, 2018, 6, 2264-2272.	5.2	163
11	Enhanced sulfide chemisorption using boron and oxygen dually doped multi-walled carbon nanotubes for advanced lithium–sulfur batteries. Journal of Materials Chemistry A, 2017, 5, 632-640.	5.2	151
12	Integrating cobalt phosphide and cobalt nitride-embedded nitrogen-rich nanocarbons: high-performance bifunctional electrocatalysts for oxygen reduction and evolution. Journal of Materials Chemistry A, 2016, 4, 10575-10584.	5.2	141
13	Na ⁺ -gated water-conducting nanochannels for boosting CO ₂ conversion to liquid fuels. Science, 2020, 367, 667-671.	6.0	136
14	Graphene Oxide Catalyzed Câ^'H Bond Activation: The Importance of Oxygen Functional Groups for Biaryl Construction. Angewandte Chemie - International Edition, 2016, 55, 3124-3128.	7.2	129
15	Biomass Valorization via Paired Electrosynthesis Over Vanadium Nitrideâ€Based Electrocatalysts. Advanced Functional Materials, 2019, 29, 1904780.	7.8	120
16	A Cu and Fe dual-atom nanozyme mimicking cytochrome c oxidase to boost the oxygen reduction reaction. Journal of Materials Chemistry A, 2020, 8, 16994-17001.	5.2	109
17	Mo2TiC2 MXene: A Promising Catalyst for Electrocatalytic Ammonia Synthesis. Catalysis Today, 2020, 339, 120-126.	2.2	102
18	A new strategy for engineering a hierarchical porous carbon-anchored Fe single-atom electrocatalyst and the insights into its bifunctional catalysis for flexible rechargeable Zn–air batteries. Journal of Materials Chemistry A, 2020, 8, 9981-9990.	5.2	97

#	Article	IF	CITATIONS
19	PtPd alloy embedded in nitrogen-rich graphene nanopores: High-performance bifunctional electrocatalysts for hydrogen evolution and oxygen reduction. Carbon, 2017, 114, 740-748.	5.4	94
20	Highly Efficient Ammonia Synthesis Electrocatalyst: Single Ru Atom on Naturally Nanoporous Carbon Materials. Advanced Theory and Simulations, 2018, 1, 1800018.	1.3	90
21	Ionothermal Synthesis of Zirconium Phosphates and Their Catalytic Behavior in the Selective Oxidation of Cyclohexane. Angewandte Chemie - International Edition, 2009, 48, 2206-2209.	7.2	89
22	Selective phenol hydrogenation to cyclohexanone over alkali–metal-promoted Pd/TiO ₂ in aqueous media. Green Chemistry, 2017, 19, 3585-3594.	4.6	88
23	Single and double boron atoms doped nanoporous C ₂ N– <i>h</i> 2D electrocatalysts for highly efficient N ₂ reduction reaction: a density functional theory study. Nanotechnology, 2019, 30, 335403.	1.3	81
24	Oxygen vacancy enhancing mechanism of nitrogen reduction reaction property in Ru/TiO2. Journal of Energy Chemistry, 2019, 39, 144-151.	7.1	79
25	A theoretical study of electrocatalytic ammonia synthesis on single metal atom/MXene. Chinese Journal of Catalysis, 2019, 40, 152-159.	6.9	76
26	Electrochemical promotion of catalysis over Pd nanoparticles for CO ₂ reduction. Chemical Science, 2017, 8, 2569-2573.	3.7	72
27	Defect engineering of nickel hydroxide nanosheets by Ostwald ripening for enhanced selective electrocatalytic alcohol oxidation. Green Chemistry, 2019, 21, 578-588.	4.6	71
28	Electrocatalytic Upgrading of Ligninâ€Đerived Bioâ€Oil Based on Surfaceâ€Engineered PtNiB Nanostructure. Advanced Functional Materials, 2019, 29, 1807651.	7.8	70
29	Recent advances in heterogeneous catalytic hydrogenation and dehydrogenation of N-heterocycles. Chinese Journal of Catalysis, 2019, 40, 980-1002.	6.9	68
30	Functionalization Ti3C2 MXene by the adsorption or substitution of single metal atom. Applied Surface Science, 2019, 465, 911-918.	3.1	63
31	Synergistic Effect of Nitrogen in Cobalt Nitride and Nitrogenâ€Ðoped Hollow Carbon Spheres for the Oxygen Reduction Reaction. ChemCatChem, 2015, 7, 1826-1832.	1.8	62
32	Point-Defect Mediated Bonding of Pt Clusters on (5,5) Carbon Nanotubes. Journal of Physical Chemistry C, 2009, 113, 890-893.	1.5	58
33	Ru nanoparticles deposited on ultrathin TiO2 nanosheets as highly active catalyst for levulinic acid hydrogenation to γ-valerolactone. Applied Catalysis B: Environmental, 2019, 259, 118076.	10.8	58
34	Mechanistic insights into the structureâ€dependent selectivity of catalytic furfural conversion on platinum catalysts. AICHE Journal, 2015, 61, 3812-3824.	1.8	53
35	Synergistic effect of S,N-co-doped mesoporous carbon materials with high performance for oxygen-reduction reaction and Li-ion batteries. Journal of Materials Chemistry A, 2015, 3, 20244-20253.	5.2	53
36	High-Throughput Screening of Hydrogen Evolution Reaction Catalysts in MXene Materials. Journal of Physical Chemistry C, 2020, 124, 13695-13705.	1.5	51

#	Article	IF	CITATIONS
37	Effects of surface functionalization of mxene-based nanocatalysts on hydrogen evolution reaction performance. Catalysis Today, 2021, 368, 187-195.	2.2	51
38	Improved Oxygen Reduction Reaction Performance of Co Confined in Ordered N-Doped Porous Carbon Derived from ZIF-67@PILs. Industrial & Engineering Chemistry Research, 2017, 56, 11100-11110.	1.8	50
39	Optimizing Alkyne Hydrogenation Performance of Pd on Carbon in Situ Decorated with Oxygen-Deficient TiO ₂ by Integrating the Reaction and Diffusion. ACS Catalysis, 2019, 9, 10656-10667.	5.5	50
40	Machine-learning-accelerated screening of hydrogen evolution catalysts in MBenes materials. Applied Surface Science, 2020, 526, 146522.	3.1	50
41	Achieving 59% faradaic efficiency of the N ₂ electroreduction reaction in an aqueous Zn–N ₂ battery by facilely regulating the surface mass transport on metallic copper. Chemical Communications, 2019, 55, 12801-12804.	2.2	45
42	Simultaneous electrochemical ozone production and hydrogen evolution by using tantalum-based nanorods electrocatalysts. Applied Catalysis B: Environmental, 2020, 266, 118632.	10.8	42
43	Hydrogen peroxide electrochemical synthesis on hybrid double-atom (Pd–Cu) doped N vacancy g-C ₃ N ₄ : a novel design strategy for electrocatalyst screening. Journal of Materials Chemistry A, 2020, 8, 2672-2683.	5.2	40
44	First-Principles Thermodynamics Study of Spinel MgAl ₂ O ₄ Surface Stability. Journal of Physical Chemistry C, 2016, 120, 19087-19096.	1.5	38
45	Double Nanoporous Structure with Nanoporous PtFe Embedded in Graphene Nanopores: Highly Efficient Bifunctional Electrocatalysts for Hydrogen Evolution and Oxygen Reduction. Advanced Materials Interfaces, 2017, 4, 1601029.	1.9	36
46	Tuning the confinement space of N-carbon shell-coated ruthenium nanoparticles: highly efficient electrocatalysts for hydrogen evolution reaction. Catalysis Science and Technology, 2017, 7, 4964-4970.	2.1	36
47	Atomic Pt Embedded in BNC Nanotubes for Enhanced Electrochemical Ozone Production via an Oxygen Intermediate-Rich Local Environment. ACS Catalysis, 2021, 11, 5438-5451.	5.5	36
48	Pyridyne cycloaddition of graphene: "external―active sites for oxygen reduction reaction. Journal of Materials Chemistry A, 2014, 2, 897-901.	5.2	33
49	Trace water triggers high-efficiency photocatalytic hydrogen peroxide production. Journal of Energy Chemistry, 2022, 64, 47-54.	7.1	33
50	Symbolic Transformer Accelerating Machine Learning Screening of Hydrogen and Deuterium Evolution Reaction Catalysts in MA ₂ Z ₄ Materials. ACS Applied Materials & Interfaces, 2021, 13, 50878-50891.	4.0	33
51	Interface hydrophobic tunnel engineering: A general strategy to boost electrochemical conversion of N2 to NH3. Nano Energy, 2022, 92, 106784.	8.2	33
52	Aqueous-Phase Acetic Acid Ketonization over Monoclinic Zirconia. ACS Catalysis, 2018, 8, 488-502.	5.5	32
53	Synergistic effect of size-dependent PtZn nanoparticles and zinc single-atom sites for electrochemical ozone production in neutral media. Journal of Energy Chemistry, 2020, 51, 312-322.	7.1	32
54	Quantitative Insights into the Reaction Mechanism for the Direct Synthesis of H ₂ O ₂ over Transition Metals: Coverage-Dependent Microkinetic Modeling. ACS Catalysis, 2021, 11, 1202-1221.	5.5	32

#	Article	IF	CITATIONS
55	Enhanced Selectivity of Phenol Hydrogenation in Low-Pressure CO ₂ over Supported Pd Catalysts. ACS Sustainable Chemistry and Engineering, 2017, 5, 11628-11636.	3.2	30
56	Role of Phenolic Groups in the Stabilization of Palladium Nanoparticles. Industrial & Engineering Chemistry Research, 2013, 52, 9783-9789.	1.8	28
57	Distinctions between Supported Au and Pt Catalysts for CO Oxidation: Insights from DFT Study. Journal of Physical Chemistry C, 2013, 117, 21331-21336.	1.5	28
58	Role of pretreatment with acid and base on the distribution of the products obtained via lignocellulosic biomass pyrolysis. RSC Advances, 2015, 5, 24984-24989.	1.7	28
59	Efficient photocatalytic reduction of CO2 using Fe-based covalent triazine frameworks decorated with in situ grown ZnFe2O4 nanoparticles. Chemical Engineering Journal, 2021, 408, 127358.	6.6	28
60	Oxygen-deficient TiO ₂ and carbon coupling synergistically boost the activity of Ru nanoparticles for the alkaline hydrogen evolution reaction. Journal of Materials Chemistry A, 2021, 9, 10160-10168.	5.2	28
61	Preparation and catalytic properties of Pd nanoparticles supported on micro-crystal DUT-67 MOFs. RSC Advances, 2015, 5, 32714-32719.	1.7	27
62	Atomically dispersed Pd catalysts in graphyne nanopore: formation and reactivity. Nanotechnology, 2017, 28, 295403.	1.3	26
63	Synergistic effect of doped nitrogen and oxygen-containing functional groups on electrochemical synthesis of hydrogen peroxide. Journal of Materials Chemistry A, 2022, 10, 4749-4757.	5.2	26
64	Lattice oxygen of PbO ₂ induces crystal facet dependent electrochemical ozone production. Journal of Materials Chemistry A, 2021, 9, 9010-9017.	5.2	25
65	Oxygen Groups Enhancing the Mechanism of Nitrogen Reduction Reaction Properties on Ru- or Fe-Supported Nb ₂ C MXene. Journal of Physical Chemistry C, 2021, 125, 14636-14645.	1.5	24
66	Palladium Dimer Supported on Mo ₂ CO ₂ (MXene) for Direct Methane to Methanol Conversion. Advanced Theory and Simulations, 2019, 2, 1800158.	1.3	22
67	Building highly active hybrid double–atom sites in C2N for enhanced electrocatalytic hydrogen peroxide synthesis. Green Energy and Environment, 2021, 6, 846-857.	4.7	22
68	In Situ Fabrication of PtCo Alloy Embedded in Nitrogenâ€Đoped Graphene Nanopores as Synergistic Catalyst for Oxygen Reduction Reaction. Advanced Materials Interfaces, 2015, 2, 1500365.	1.9	21
69	Synergetic effect of pyrrolic-N and doped boron in mesoporous carbon for electrocatalytic ozone production. Journal of Materials Chemistry A, 2020, 8, 2336-2342.	5.2	21
70	Graphene Oxide Catalyzed Câ^'H Bond Activation: The Importance of Oxygen Functional Groups for Biaryl Construction. Angewandte Chemie, 2016, 128, 3176-3180.	1.6	20
71	CO Oxidation by Lattice Oxygen on V ₂ O ₅ Nanotubes. Journal of Physical Chemistry C, 2011, 115, 14806-14811.	1.5	19
72	A radar-like iron based nanohybrid as an efficient and stable electrocatalyst for oxygen reduction. Journal of Materials Chemistry A, 2014, 2, 6703-6707.	5.2	18

#	Article	IF	CITATIONS
73	The Effect of N ontaining Supports on Catalytic CO Oxidation Activity over Highly Dispersed Pt/UiOâ€67. European Journal of Inorganic Chemistry, 2017, 2017, 172-178.	1.0	18
74	Hydrogen peroxide synthesis on porous graphitic carbon nitride using water as a hydrogen source. Journal of Materials Chemistry A, 2020, 8, 124-137.	5.2	18
75	Position of substituent dependent dimensionality in Ln–Cu heterometallic coordination polymers. CrystEngComm, 2012, 14, 679-683.	1.3	16
76	Synthesis, properties, and magnetism–structure relationship of lanthanide-based metal–organic frameworks with (ethylenedithio)acetic acid. CrystEngComm, 2014, 16, 6963.	1.3	16
77	Enhanced Catalytic Performances for Guaiacol Aqueous Phase Hydrogenation over Ruthenium Supported on Mesoporous TiO ₂ Hollow Spheres Embedded with SiO ₂ Nanoparticles. ChemistrySelect, 2017, 2, 9599-9606.	0.7	16
78	Twin-like ternary PtCoFe alloy in nitrogen-doped graphene nanopores as a highly effective electrocatalyst for oxygen reduction. Catalysis Science and Technology, 2016, 6, 5942-5948.	2.1	15
79	Dual effect of the coordination field and sulphuric acid on the properties of a single-atom catalyst in the electrosynthesis of H ₂ O ₂ . Physical Chemistry Chemical Physics, 2021, 23, 21338-21349.	1.3	15
80	Geometric and electronic effects on the performance of a bifunctional Ru2P catalyst in the hydrogenation and acceptorless dehydrogenation of N-heteroarenes. Chinese Journal of Catalysis, 2021, 42, 1185-1194.	6.9	14
81	Pd-Co alloy supported on TiO2 with oxygen vacancies for efficient N2 and O2 electrocatalytic reduction. Applied Surface Science, 2021, 567, 150680.	3.1	14
82	Transition of chemically modified diphenylalanine peptide assemblies revealed by atomic force microscopy. RSC Advances, 2014, 4, 7516.	1.7	13
83	Effect of graphene with nanopores on metal clusters. Physical Chemistry Chemical Physics, 2015, 17, 24420-24426.	1.3	13
84	Multiscale Simulation on Product Distribution from Pyrolysis of Styrene-Butadiene Rubber. Polymers, 2019, 11, 1967.	2.0	13
85	The effect of earth metal ion on the property of peptide-based metal–organic frameworks. CrystEngComm, 2013, 15, 5545.	1.3	12
86	Waste Tire Pyrolysis for the Production of Light Hydrocarbons over Layered Catalysts. Energy Technology, 2015, 3, 851-855.	1.8	12
87	High-performance single-atom Ni catalyst loaded graphyne for H2O2 green synthesis in aqueous media. Journal of Colloid and Interface Science, 2021, 599, 58-67.	5.0	12
88	Engineering the geometric and electronic structure of Ru <i>via</i> Ru–TiO ₂ interaction for enhanced selective hydrogenation. Catalysis Science and Technology, 2022, 12, 1005-1016.	2.1	12
89	Water oxidation on Nâ€Doped TiO ₂ nanotube arrays. International Journal of Quantum Chemistry, 2012, 112, 2585-2590.	1.0	10
90	Experimental, DFT and quantum Monte Carlo studies of a series of peptide-based metal–organic frameworks: synthesis, structures and properties. Inorganic Chemistry Frontiers, 2014, 1, 526-533.	3.0	10

#	Article	IF	CITATIONS
91	CO oxidation over supported <scp>P</scp> t clusters at different <scp>CO</scp> coverage. International Journal of Quantum Chemistry, 2016, 116, 939-944.	1.0	10
92	Fe(CN) ₅ @PIL-derived N-doped porous carbon with FeC _x N _y active sites as a robust electrocatalyst for the oxygen reduction reaction. Catalysis Science and Technology, 2019, 9, 97-105.	2.1	10
93	Micromechanical simulation of the pore size effect on the structural stability of brittle porous materials with bicontinuous morphology. Physical Chemistry Chemical Physics, 2019, 21, 12895-12904.	1.3	10
94	2D-3D transformation of palladium and gold nanoparticles on functionalized Mo2C by multiscale simulation. Applied Surface Science, 2019, 481, 554-563.	3.1	10
95	A generalized formula for two-dimensional diffusion of CO in graphene nanoslits with different Pt loadings. Green Energy and Environment, 2020, 5, 322-332.	4.7	10
96	A first-principles study of reaction mechanism over carbon decorated oxygen-deficient TiO2 supported Pd catalyst in direct synthesis of H2O2. Chinese Journal of Chemical Engineering, 2021, 31, 126-134.	1.7	10
97	Weak Pb–O of confined [Pb–O ₄] in pyramidal sillenite-type Bi ₁₂ PbO ₂₀ for enhanced electrochemical ozone production. Journal of Materials Chemistry A, 2022, 10, 5430-5441.	5.2	10
98	Enhanced Oxygen Reduction Activity on Carbon Supported Pd Nanoparticles Via SiO ₂ . ChemCatChem, 2019, 11, 1278-1285.	1.8	9
99	Ultrathin 2D flower-like CoP@C with the active (211) facet for efficient electrocatalytic water splitting. CrystEngComm, 2021, 23, 1777-1784.	1.3	9
100	Synergistic Effect of Coordination Fields and Hydrosolvents on the Single-Atom Catalytic Property in H ₂ O ₂ Synthesis: A Density Functional Theory Study. Journal of Physical Chemistry C, 2022, 126, 2349-2364.	1.5	9
101	Computational screening of O-functional MXenes for electrocatalytic ammonia synthesis. Chinese Journal of Catalysis, 2022, 43, 1860-1869.	6.9	9
102	Multiscale Simulation of Morphology Evolution of Supported Pt Nanoparticles via Interfacial Control. Langmuir, 2019, 35, 6393-6402.	1.6	8
103	Additives initiate selective production of chemicals from biomass pyrolysis. Bioresource Technology, 2014, 156, 376-379.	4.8	7
104	Effect of Crossâ€Linked Structures on Mechanical Properties of Styreneâ€Butadiene Rubber via Molecular Dynamics Simulation. Macromolecular Theory and Simulations, 2022, 31, 2100054.	0.6	7
105	Multiphysics modeling of proton exchange membrane water electrolysis: From steady to dynamic behavior. AICHE Journal, 2022, 68, .	1.8	7
106	Lattice Oxygen of PbO ₂ (101) Consuming and Refilling via Electrochemical Ozone Production and H ₂ O Dissociation. Journal of Physical Chemistry C, 2022, 126, 8627-8636.	1.5	7
107	BrĄ̃nsted–Evans–Polanyi Relations for H2O2 Synthesis on Gold Surfaces. Catalysis Letters, 2012, 142, 601-607.	1.4	6
108	Density functional theory study of <i>p</i> â€chloroaniline adsorption on Pd surfaces and clusters. International Journal of Quantum Chemistry, 2014, 114, 895-899.	1.0	6

#	Article	IF	CITATIONS
109	Ru Cluster-Decorated Cu Nanoparticles Enhanced Selectivity to Imine from One-Pot Cascade Transformations. Industrial & Engineering Chemistry Research, 2022, 61, 3474-3482.	1.8	6
110	Meso-scale simulation on mechanism of Na+-gated water-conducting nanochannels in zeolite NaA. Journal of Membrane Science, 2021, 635, 119462.	4.1	5
111	Sintering Rate and Mechanism of Supported Pt Nanoparticles by Multiscale Simulation. Langmuir, 2021, 37, 12529-12538.	1.6	5
112	Reaction and Transport Co-Intensification Enhanced Continuous Flow Electrocatalytic Aminoxyl-Mediated Oxidation of Sterol Intermediates by 3D Porous Framework Electrode. Chemical Engineering Journal, 2022, , 136659.	6.6	5
113	Oxygen vacancies on Nb ₂ O ₅ enhanced the performance of H ₂ O ₂ electrosynthesis from O ₂ reduction. Chemical Communications, 2022, 58, 8428-8431.	2.2	5
114	Unravelling the functional complexity of oxygen-containing groups on carbon for the reduction of NO with NH3. Journal of the Taiwan Institute of Chemical Engineers, 2022, 133, 104261.	2.7	4
115	Rücktitelbild: Graphene Oxide Catalyzed Câ^'H Bond Activation: The Importance of Oxygen Functional Groups for Biaryl Construction (Angew. Chem. 9/2016). Angewandte Chemie, 2016, 128, 3290-3290.	1.6	3
116	Effect of Hydrogen-Induced Metallization on Chemisorption. Journal of Physical Chemistry C, 2019, 123, 15171-15175.	1.5	3
117	Multiscale simulation on thermal stability of supported metal nanocatalysts. Wiley Interdisciplinary Reviews: Computational Molecular Science, 2019, 9, e1405.	6.2	3
118	MoO _{<i>x</i>} Nanoparticle Catalysts for <scp>d</scp> -Glucose Epimerization and Their Electrical Immobilization in a Continuous Flow Reactor. ACS Applied Materials & Interfaces, 2019, 11, 44118-44123.	4.0	2
119	High-efficiency visible-light photocatalytic H ₂ O ₂ production using CdSe-based core/shell quantum dots. Catalysis Science and Technology, 2022, 12, 2865-2871.	2.1	2
120	Enhanced oxygen reduction reaction performance over Pd catalysts by oxygen-surface-modified SiC. Chinese Journal of Catalysis, 2021, 42, 963-970.	6.9	1